

The Distribution of the Equivalent Stresses in the Dangerous Section of the Strength Elements Made by U - Profile with Thin Walls *

Vékonyfalú „U” profilok veszélyes keresztmetszeteinek feszültségeloszlásának elemzése

Galaftion SOFONEA¹, Marcu FRĂȚILĂ², Constantin VASILOAICA³

Keywords: thin walls sections, stresses, optimization, hindrance twist.

Kulcsszavak: vékonyfalú profilok, feszültség, optimalizálás, gátolt csavarás

Összefoglalás

A veszélyes keresztmetszetekben lévő ekvivalens feszültségek változásának vizsgálata hatékonyabb anyagkihasználást tesz lehetővé, ami akár 10 % körüli anyagmegtakarítást jelenthet. A számított és kísérletileg meghatározott feszültségek közötti eltérés 5 - 15,4 %, 7,5 % körüli átlagos hiba mellett. Kisebb feszültségek mellett nagyobb hibák adódnak. A gátolt csavarás esetében ezek a hibák nagyobbak. A ténylegesen mért feszültségek általában nagyobbak a számítással meghatározottaknál. Mind a számításnál, mind pedig a kísérleteknél egy egyszerűsített feltevést is figyelembe véve, a kapott hibák nagysága elfogadható mértékű és így a kapott eredmények kiterjeszthetők más keresztmetszet alakokra és terhelési esetekre is.

Summary

The work presents the research on the optimization of the material distribution on the thin wall sections made by the U profile taking into consideration the sections dimensions, by maintaining the same area. The variation diagrams of the sections geometrical characteristics are shown below as well as the distribution of the equivalent stresses in the dangerous segment taking into consideration also the hindrance twist.

* A 24. Duna-Adria Szimpóziumon elhangzott előadás szerkesztett változata

1,2,3 University “Lucian Blaga” of Sibiu, “Hermann Oberth” Engineering Faculty, Romania

1-galaftion.sofonea@ulbsibiu.ro,

2-marcu.fratila@ulbsibiu.ro,

3-constantin.vasiloaica@ulbsibiu.ro

1. Notes and terminology

- b – section's width, [mm];

- h – section's height, [mm];

- l, l_1, l_2 - rad's length, [mm];

- t – the wall's thickness, [mm];

$$k^2 = \frac{G \cdot I_t}{E \cdot I_\omega}, [\text{mm}^2];$$

- I_t - the geometrical characteristic of pure twist rigidity, $[\text{mm}^4]$;

- I_z - axial inertia moment compared to the Oz axis, $[\text{mm}^4]$;

- I_ω - sector inertia moment, $[\text{mm}^6]$;

- S_ω - static sector moment, $[\text{mm}^4]$.

- B_ω - bimoment, $[N \cdot \text{mm}^2]$;

- N – axial force, $[N]$;

- M_z, M_y - bending moments, $[N \cdot \text{mm}]$;

- M_t - pure twisting moment, $[N \cdot \text{mm}]$;

- M_ω - twisting-bending moment, $[N \cdot \text{mm}]$;

- E, G - longitudinal, transversal module, $[\text{MPa}]$;

- T_y, T_z - cutting forces, $[N]$;

- σ, τ - normal, tangential stresses, $[\text{MPa}]$;

- ω - sector coordinate, $[\text{mm}^2]$.

2. Geometrical characteristics

In the Figures 1 - 5 are shown characteristics of the geometrical sections.

$$a_z = \frac{b^2 \cdot t_1}{2 \cdot b \cdot t_1 + \frac{h \cdot t_2}{3}} \quad (1)$$

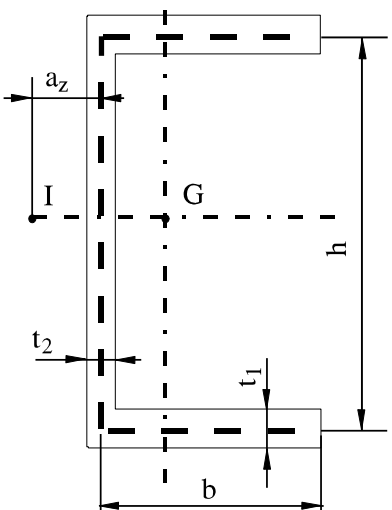


Fig. 1 Geometrical dimensions
1. ábra Geometriai méretek

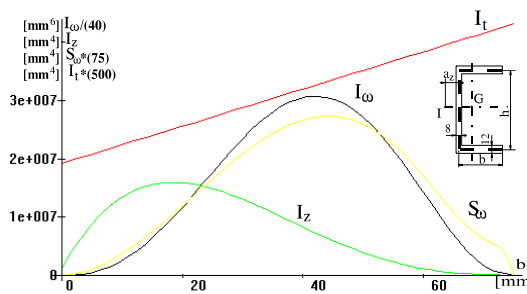


Fig. 2 The variation diagram of geometrical characteristics for $A=1800 \text{ [mm}^2]$, $t_1=12 \text{ [mm]}$; $t_2=8 \text{ [mm]}$

2. ábra A geometriai jellemzők változási diagramja $A=1800 \text{ [mm}^2]$, $t_1=12 \text{ [mm]}$; $t_2=8 \text{ [mm]}$ esetére

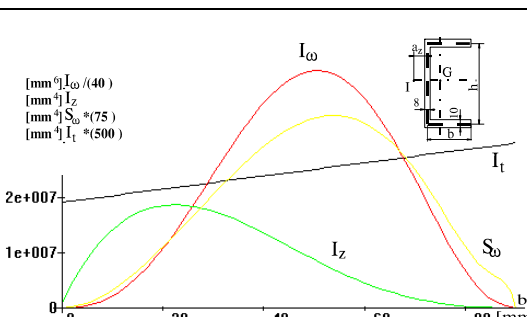


Fig. 3 The variation diagram of geometrical characteristics for $A=1800 \text{ [mm}^2]$, $t_1=10 \text{ [mm]}$; $t_2=8 \text{ [mm]}$

3. ábra A geometriai jellemzők változási diagramja $A=1800 \text{ [mm}^2]$, $t_1=10 \text{ [mm]}$; $t_2=8 \text{ [mm]}$ esetére

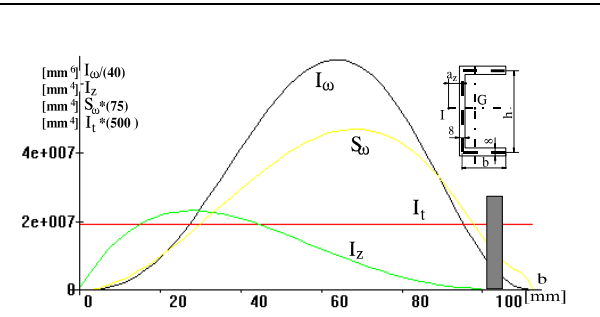


Fig. 4 The variation diagram of geometrical characteristics for $A=1800 \text{ [mm}^2]$, $t_1=8 \text{ [mm]}$; $t_2=8 \text{ [mm]}$.

4. ábra A geometriai jellemzők változási diagramja $fA=1800 \text{ [mm}^2]$, $t_1=8 \text{ [mm]}$; $t_2=8 \text{ [mm]}$ esetére

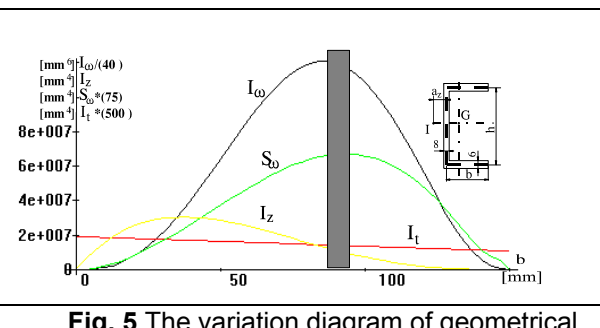


Fig. 5 The variation diagram of geometrical characteristics for $A=1800 \text{ [mm}^2]$, $t_1=6 \text{ [mm]}$; $t_2=8 \text{ [mm]}$.

5. ábra A geometriai jellemzők változási diagramja $A=1800 \text{ [mm}^2]$, $t_1=6 \text{ [mm]}$; $t_2=8 \text{ [mm]}$ esetére

$$I_t = \frac{1}{3} \cdot (2 \cdot b \cdot t_1^3 + h \cdot t_2^3); \quad (2)$$

$$I_z = \frac{\left(b + \frac{t_2}{2} \right) \cdot (h + t_1)^3 - \left(b - \frac{t_2}{2} \right) \cdot (h - t_1)^3}{12}; \quad (3)$$

$$S_{\omega \max} = \frac{h \cdot (b - a_z)^2}{4} \cdot t_1 \quad (4)$$

The variation of this geometrical characteristics are shown for $A=1800 \text{ [mm}^2]$, and $t_1=8; 10; 12 \text{ [mm]}$; $t_2=6; 8 \text{ [mm]}$.

Local stability condition [6] for sole of profile is:

$$\frac{b}{t_1} \leq k_1, \quad (5)$$

where $k=13$.

3. General considerations

The analysis of strength elements realised from U shaped iron profiles, for different loads and connections takes into account the distribution of equivalent stresses in the dangerous cross-section, considering also the blocked torsion. This analysis is carried out for various cross-sections, the area remaining constant [5].

The mathematical solution to this optimization problem would be the most indicated way, offering remarkable advantages, but such an approach is not always accessible in the case of strength structures because it must take into consideration a number of factors, objective and subjective ones.

The calculation relations for bars made of thin walled open profiles, taking into account also the blocked torsion are:

$$\sigma = \frac{M_z \cdot I_y + M_y \cdot I_{zy}}{I_y \cdot I_z - I_{zy}^2} \cdot y - \frac{M_y \cdot I_z + M_z \cdot I_{zy}}{I_z \cdot I_y - I_{zy}^2} \cdot z + \frac{N}{A} + \frac{B_\omega}{I_\omega} \cdot \alpha \quad (6)$$

$$\tau = \frac{T_y \cdot I_z - T_z \cdot I_y}{b(I_y \cdot I_z - I_{zy}^2)} \cdot S_z + \frac{T_z \cdot I_z - T_y \cdot I_y}{h(I_y \cdot I_z - I_{zy}^2)} \cdot S_y + \frac{M}{I_d} \cdot t + \frac{M_\omega}{t \cdot I_\omega} \cdot S_\omega \quad (7)$$

For bars made of thin walled open profiles, loading with a excentrical force in relation with symmetrical longitudinal axis the static size and geometrical size are:

- for interval $0 \leq x \leq t_p$:

$$\begin{bmatrix} \phi(x) \\ \phi'(x) \\ B(x) \\ G \cdot I_t \\ M(x) \end{bmatrix} = \begin{bmatrix} 1 & \frac{1}{k} \cdot shkx & 1 - chkx & x - \frac{1}{k} \cdot shkx \\ 0 & chkx & -k \cdot shkx & 1 - chkx \\ 0 & -\frac{1}{k} \cdot shkx & chkx & \frac{1}{k} \cdot shkx \\ 0 & 0 & 0 & 1 \end{bmatrix} \cdot \begin{bmatrix} \phi_0 \\ \phi'_0 \\ B_0 \\ G \cdot I_t \\ M_{x0} \end{bmatrix} \quad (8)$$

- for interval $t_p \leq x \leq l$:

$$\begin{bmatrix} \phi(x) \\ \phi'(x) \\ B(x) \\ G \cdot I_t \\ M(x) \end{bmatrix} = \begin{bmatrix} 1 & \frac{1}{k} \cdot shkx & 1 - chkx & x - \frac{l}{k} \cdot shkx & \frac{l}{k} \cdot shk(x-t_p) - (x-t_p) \\ 0 & chkx & -k \cdot shkx & 1 - chkx & chk(x-t_p) - 1 \\ 0 & -\frac{1}{k} \cdot shkx & chkx & \frac{l}{k} \cdot shkx & -\frac{l}{k} \cdot shk(x-t_p) \\ 0 & 0 & 0 & 1 & -1 \end{bmatrix} \cdot \begin{bmatrix} \phi_0 \\ \phi'_0 \\ B_0 \\ G \cdot I_t \\ M_{x0} \\ G \cdot I_t \\ P_e \\ G \cdot I_t \end{bmatrix} \quad (9)$$

The strength condition imposed according to the theory of shape variation energy is:

$$\sigma_{ech} = \sqrt{\sigma^2 + 3 \cdot \tau^2} \leq \sigma_a \quad (10)$$

4. Variation of equivalent stresses in the dangerous cross-section

The developed software programme allows the dimensioning by successive trials, so that condition (3) is observed, as well as the drawing of the equivalent stresses' variation in the most solicited cross-section points for $A=\text{const}$, when the width and the height h vary, maintaining the area constant [1]. These variations of the equivalent stresses for an actual case of loading are given in Figures 6...9.

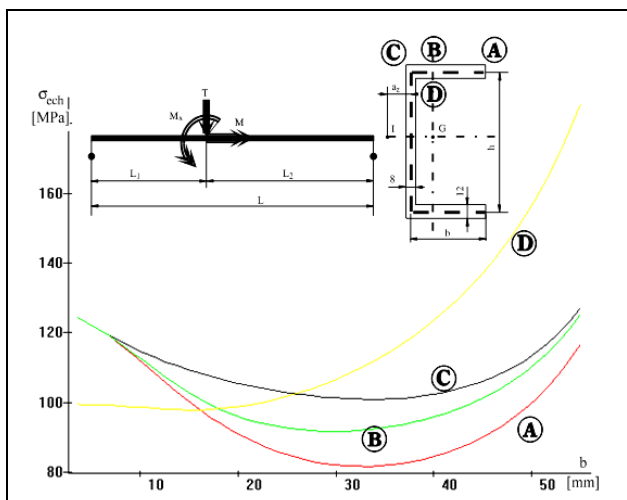


Fig. 6 The variation diagram of analytically determined equivalent stresses

$A=1800 \text{ [mm}^2]$, $t_1=12 \text{ [mm]}$; $t_2=8 \text{ [mm]}$

6. ábra Az analitikusan meghatározott ekvivalens feszültség változási diagramja $A=1800 \text{ [mm}^2]$, $t_1=12 \text{ [mm]}$; $t_2=8 \text{ [mm]}$

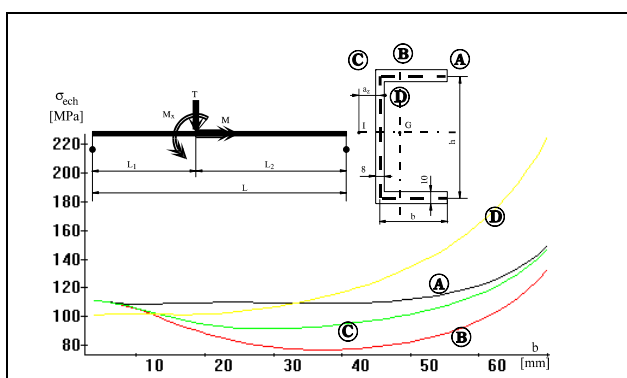


Fig. 7 The variation diagram of analytically determined equivalent stresses

$A=1800 \text{ [mm}^2]$, $t_1=10 \text{ [mm]}$; $t_2=8 \text{ [mm]}$.

7. ábra Az analitikusan meghatározott ekvivalens feszültség változási diagramja $A=1800 \text{ [mm}^2]$, $t_1=10 \text{ [mm]}$; $t_2=8 \text{ [mm]}$

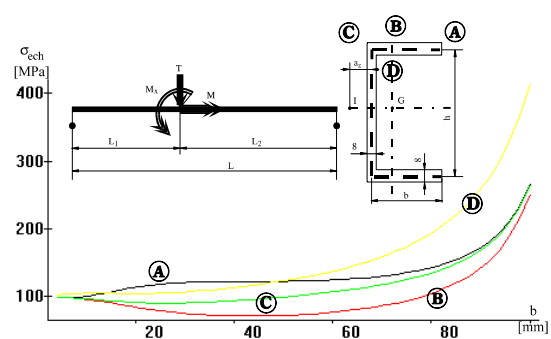


Fig. 8 The variation diagram of analytically determined equivalent stresses $A=1800 \text{ [mm}^2]$, $t_1=8 \text{ [mm]}$; $t_2=8 \text{ [mm]}$

8. ábra Az analitikusan meghatározott ekvivalens feszültség változási diagramja $A=1800 \text{ [mm}^2]$, $t_1=8 \text{ [mm]}$; $t_2=8 \text{ [mm]}$

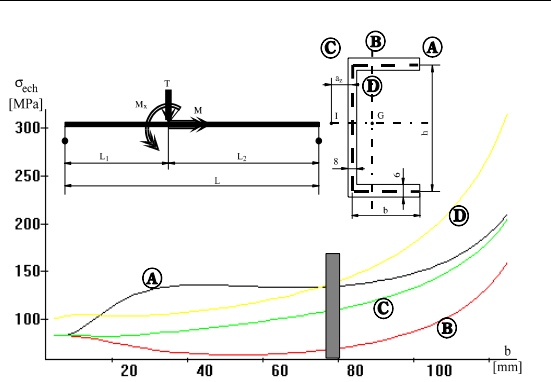


Fig. 9 The variation diagram of analytically determined equivalent stresses $A=1800 \text{ [mm}^2]$, $t_1=6 \text{ [mm]}$; $t_2=8 \text{ [mm]}$

9. ábra Az analitikusan meghatározott ekvivalens feszültség változási diagramja $A=1800 \text{ [mm}^2]$, $t_1=6 \text{ [mm]}$; $t_2=8 \text{ [mm]}$

Beneath the theoretical solutions obtained and shown in Figure 1, also local stability conditions must be imposed for the sole and the heart (hatched rectangle).

For the optimal solutions for realising the U profile, the normal and tangential stresses were determined theoretically and experimentally.

5. Experimental determinations of normal and tangential stresses

For this purpose, a device was designed and realised that allows the mounting and loading of thin-walled bars made from U profile with transversal loads applied centrically or excentrically with regard to the axis of the bending-torsion centre.

Also, this device allows the simulation of various types of joints, from the fork type support to the rigid constraining (Fig. 10).

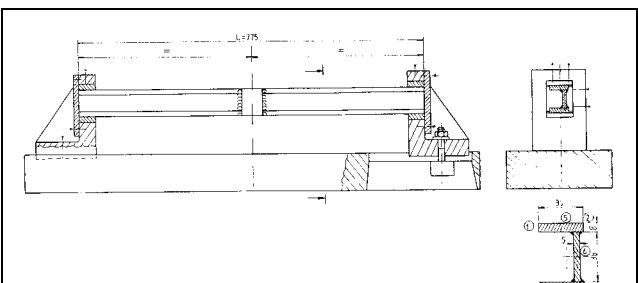


Fig. 10 Testing device
10. ábra Vizsgáló berendezés

For determining the stresses, resistive tensometrical transducers were used, their placement scheme being shown in Fig. 11.

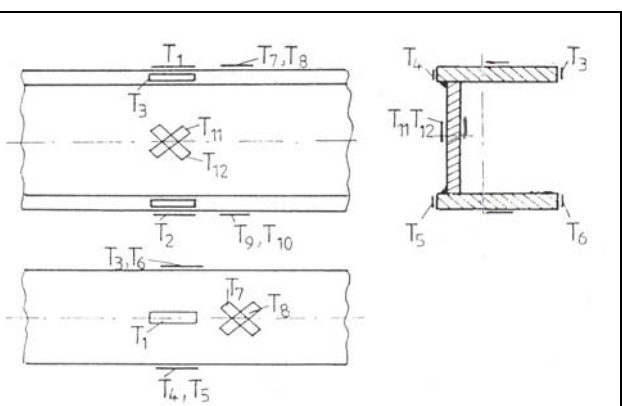


Fig. 11 Placement scheme of the resistive transducers
11. ábra A nyúlásmérő bélyegek elhelyezése

The determination of normal stresses was done with transducers T1-T2 connected as a semi-bridge, while the stresses ω σ in the profile's soles was done with the transducers T3, T4 and T5, T6, respectively, also connected as semi-bridge. The testing of tangential stresses was done with the 189 transducers T7, T8, T9, T10 and T11, T12, T13, T14, respectively, connected in full bridges.

The experimental tests were carried out on a testing machine Fig. 12.

The comparative values of these stresses, for various loads and load eccentricities, as well as the displaying of the differences between the theoretical and experimental values are shown in Fig. 13 and 14.



Fig.12 Strain gauges
12. ábra Nyúlmérő béllyegek

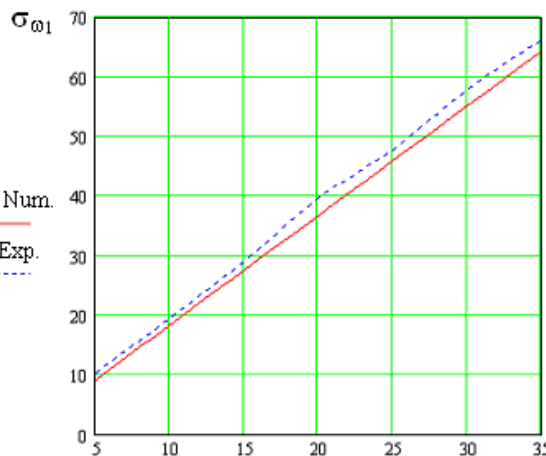


Fig. 13 Theoretical and experimental values of stresses $\sigma_{\omega 1}$
13. ábra A $\sigma_{\omega 1}$ feszültségek elméleti és mért értékei

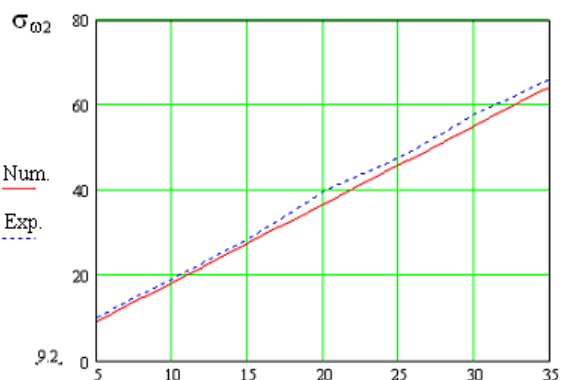


Fig. 14 Theoretical and experimental values of stresses $\sigma_{\omega 2}$
14. ábra A $\sigma_{\omega 2}$ feszültségek elméleti és mért értékei

6. Conclusions

The analysis of variation of equivalent stresses in the dangerous section allows a more efficient usage of the material, gaining savings of about 10%.

The differences between calculated and experimentally determined stresses are in the range of 5...15.4%, with average errors of about 7.5%.

The errors are the larger as the stresses are smaller.

Also, these errors are larger for stresses produced by the blocked torsion ($\omega \omega \sigma_{,\tau}$).

Also, it can be noticed that, usually, the stresses obtained experimentally are larger than the ones resulted from analytical calculations. Taking into account the simplifying hypotheses, both for theoretical calculations and for experimental determinations, the resulted errors are acceptable and therefore this comparative study can be extended also to other cross-section shapes or to other load types.

Bibliography

- [1] Boleanțu, L., Sofonea, G., Optimizarea secțiunilor profil deschis utilizate la construcția de utilaje grele, A XII-a Conferință de mecanica solidului, Sibiu, 1989
- [2] Kollbrunner, C. F., Hajdin, N., Wolbkrafttorsion dunnwandiger Stabe mit offenem Profil, Teil I, Schweizer Stahlbau-Vereinigung Zurich, nr. 29, 1964.
- [3] Kollbrunner, C. F., Hajdin, N., Wolbkrafttorsion dunnwandiger Stabe mit offenem Profil, Teil II, Schweizer Stahlbau-Vereinigung Zurich, nr. 29, 1965.
- [4] Petre, A., Calculul structurilor de aviație, Ed. Tehnică, București, 1984
- [5] Sofonea, G., The distribution of the equivalent stresses in the dangerous section of strength elements in made bz U – profile with thin walls, Proceedings TMT 2006, 10th International Research / Expert Conference „ Trends in the Development of Machinery and Associated Technology”, pag. 905 - 908, 11-14 September 2006, Barcelona-Lloret de Mar, Spain, ISBN 9958 – 617 – 30 – 7;
- [6] Sofonea, G., Optimizarea distribuției de material pe secțiunile barelor cu pereți subțiri – profil cheson simetric, Revista Căilor Ferate Române, nr. 4, 1992. [7] Sofonea, G., Blezu, D., Optimizarea structurilor de rezistență realizate din bare cu pereți subțiri, I.I.S. Sibiu, 1990.